Expression, characterization and crystal structure of thioredoxin from *Schistosoma japonicum*

YONGDONG LI[1,2,3], PAN LI[2], YUN PENG[2], QUNFENG WU[1,2,3], FUYAN HUANG[2], XIANG LIU[2], XUN LI[2], HUI ZHOU[2], DAOYI GUO[2], DASHUANG SHI[2,4], XIAO-NONG ZHOU[1,3]* *and* XIAOLIN FAN[2]*

[1] *National Institute of Parasitic Diseases, Chinese Center for Disease Control and Prevention, Shanghai 200025, People's Republic of China*
[2] *Key Laboratory of Organo-Pharmaceutical Chemistry, Jiangxi Province, Chemistry and Chemical Engineering College, Gannan Normal University, Ganzhou 341000, People's Republic of China*
[3] *Key Laboratory on Biology of Parasite and Vector, Ministry of Health, and WHO Collaborating Center for Malaria, Schistosomiasis and Filariasis, Shanghai 200025, People's Republic of China*
[4] *Center for Genetic Medicine Research and Department of Integrative Systems Biology, Children's National Medical Center, The George Washington University, Washington, District of Columbia 20010, USA*

(*Received 3 December 2014; revised 6 February 2015; accepted 19 February 2015; first published online 26 March 2015*)

SUMMARY

Schistosoma japonicum, a human blood fluke, causes a parasitic disease affecting millions of people in Asia. Thioredoxin–glutathione system of *S. japonicum* plays a critical role in maintaining the redox balance in parasite, which is a potential target for development of novel antischistosomal agents. Here we cloned the gene of *S. japonicum* thioredoxin (SjTrx), expressed and purified the recombinant SjTrx in *Escherichia coli*. Functional assay shows that SjTrx catalyses the dithiothreitol (DTT) reduction of insulin disulphide bonds. The coupling assay of SjTrx with its endogenous reductase, thioredoxin glutathione reductase from *S. japonicum* (SjTGR), supports its biological function to maintain the redox homeostasis in the cell. Furthermore, the crystal structure of SjTrx in the oxidized state was determined at 2·0 Å resolution, revealing a typical architecture of thioredoxin fold. The structural information of SjTrx provides us important clues for understanding the maintenance function of redox homeostasis in *S. japonicum* and pathogenesis of this chronic disease.

Key words: thioredoxin, crystal structure, *Schistosoma japonicum*.

INTRODUCTION

Schistosomiasis is an important parasitic disease in humans, affecting more than 78 countries including 52 endemic countries with moderate to high transmission in the world, in which at least 249 million people required preventive treatment in 2012 (WHO, 2014). *Schistosoma japonicum* is one of species of oriental schistosome, surviving in veins of the final host for many years without elimination from the attack of host immune system (Capron and Capron, 1986). Previous studies indicated that the oxidative stress from reactive oxygen species (ROS), which mainly produced by host effector cells (eosinophils and macrophages) adhering to the antibody-coated worms, results in haemoglobinolytic process, which is highly toxic to schistosome (Butterworth, 1984; Ryter and Tyrrell, 2000). However, antioxidants from schistosome might remove the ROS generated in veins and released from host immune cells to protect worms from oxidative damage (Kazura *et al*. 1981; Butterworth, 1984; Loverde, 1998; Liu Jian *et al*. 2012). These antioxidant proteins in thiol-mediated detoxification pathway mainly include two redox molecules: one is glutathione (GSH), and the other one is thioredoxin (Trx). In schistosome, electrons from NADPH are transferred via an oxidoreductase flavoenzyme of thioredoxin glutathione reductase (TGR) using these two molecules: GSH and Trx (Alger and Williams, 2002; Kuntz *et al*. 2007).

Thiol-mediated detoxification reactions in two parallel pathways in mammals play an important role for redox homeostasis in the cell (Hatahet and Ruddock, 2009; Jensen *et al*. 2009). As a protein disulphide oxidoreductases, Trx is involved in a large variety of cellular redox reactions, in which electrons flow from NADPH through redox protein of thioredoxin reductase (TrxR) to final oxidant molecules. In addition to the function of antioxidant defence, Trx has also been implicated in protein folding, DNA repair and synthesis, transcription regulation and cell growth (Arner and Holmgren, 2000; Powis & Montfort, 2001; Kaimul Ahsan *et al*. 2005;

* Corresponding authors. Key Laboratory on Biology of Parasite and Vector, Ministry of Health, and WHO Collaborating Center for Malaria, Schistosomiasis and Filariasis, Shanghai 200025, People's Republic of China, Key Laboratory of Organo-Pharmaceutical Chemistry, Jiangxi Province, Chemistry and Chemical Engineering College, Gannan Normal University, Ganzhou 341000, People's Republic of China. E-mail: fanxl2002@yahoo.com.cn and xiaonongzhou1962@gmail.com

doi:10.1017/S0031182015000244

Michelet *et al*. 2005; Yoshioka *et al*. 2006; Lillig and Holmgren, 2007). Trx is a small (about 12 kDa) protein with a redox active disulphide in the conserved motif of Trp–Cys–Gly–Pro–Cys (WCGPC). In the oxidized state, the disulphide (Trx-S_2) is formed between two cysteine residues in the sequence of WCGPC. Subsequently, the oxidized Trx is reduced back to the dithiol form of [Trx-$(SH)_2$] by TrxR and NADPH (Wahl *et al*. 2005). For the thioredoxin-dependent redox cycle in schistosome, the TrxR was replaced by TGR (Alger and Williams, 2002; Kuntz *et al*. 2007; Han *et al*. 2012; Song *et al*. 2012).

In this study, we present the work on gene cloning, protein expression in *E. coli*, purification and functional characterization of the *S. japonicum* thioredoxin (SjTrx). We also determined the crystal structure of the oxidized state SjTrx, showing a typical tertiary fold of Trx superfamily proteins.

MATERIALS AND METHODS

Materials

A female *S. japonicum* cDNA library was kindly provided by Dr Chen from National Institute of Parasitic Disease, Chinese Center for Disease and Prevention. Recombinant SjTGR containing an N-terminal six-histidine tag was prepared in our laboratory. CloExpress One Step Cloning Kit was purchased from Vazyme Biotech Co., Ltd. Others kits were purchased from Sangon Biotech (Shanghai) Co., Ltd. All reagents were of the highest purity available.

Cloning, codon optimization and construction of plasmids

The protein sequence of SjTrx was identified by searching NCBI database. The corresponding cDNA sequence of GenBank AF091538·1 was used to design primers for gene amplification. The open reading frame of DNA fragment encoding SjTrx was amplified by the polymerase chain reaction (PCR) using the female *S. japonicum* cDNA library as the template and a pair of gene specific primers (forward primer, 5′-GTGCCGCGCGG CAGCCATATGAGTAACGTACTGCATATA GA and reverse primer, 5′-ACGGAGCTCGAA TTCGGATCCTCATTTGTGTTTCCGGAT).

To improve the yield of SjTrx protein, codon optimization for expression in *E. coli* was carried out based on the SjTrx full-length gene using the web server of Optimizer (Puigbo *et al*. 2007, 2008). The optimized SjTrx gene was synthesized directly (Qinglan Biological Technology Co., Ltd).

Both native and optimized SjTrx genes were then cloned into a pET28a commercial vector (Novagen) to obtain an N-terminal His-tag fused protein using *Nde* and *BamH* sites. The SjTrx gene insertions in the expression vector SjTrx-pET28a were confirmed by DNA sequencing at Sangon Corporation.

Expression and purification of SjTrx

Both native and optimized SjTrx-pET28a plasmids were transformed into *E. coli* BL21 (DE3) competent cells according to the manufacturer's instructions. Cells containing corresponding plasmid were grown in 20 mL of Luria-Bertani (LB) medium containing kanamycin (50 μg mL^{-1}) with shaking at 37 ° C overnight. Cultures were then transferred into 1 L of LB medium containing 50 μg mL^{-1} of kanamycin and grown at 37°. When the absorbance value of the bacteria culture at 600 nm reached 1·0, isopropylthiogalactoside (IPTG) was added to a final concentration of 0·2 mM to induce the expressions of SjTrx. Cells were then grown at 25 °C for 24 h.

Bacteria cells were collected by centrifugation at 12 000 ***g*** and suspended in about 20 mL of the Ni-affinity lysis buffer (300 mM NaCl, 50 mM NaH_2PO_4, pH 7·4). Cells were disrupted by sonication on ice 4 times with 40 s each time at maximum power. Cellular debris was removed by centrifugation for 30 min at 13 000 ***g*** and passing through a 0·45 μm filter. The protein was purified using Histrap Ni-affinity column (GE Healthcare) and then Hitrap DEAE column (GE Healthcare) on an AKTA UPC-10 system. At first, the resulting soluble fraction was loaded onto a 5 mL Histrap Ni-affinity column equilibrated with lysis buffer. Then the column was washed with the buffer containing 50 mM imidazole and finally the protein was eluted with the buffer containing 250 mM imidazole. The protein was then dialyzed into a buffer containing 50 mM NaCl, 20 mM Tris-HCl (pH 8·0) and 1 mM EDTA and loaded onto a DEAE Hitrap column. The final pure protein was eluted with the linear gradient method using a buffer of 500 mM NaCl, 20 mM Tris-HCl (pH 8·0), 1 mM EDTA. In addition, 5 mM of β-mercaptoethanol was added into buffers for the preparation of the reduced state protein. Protein purity was assessed by SDS-PAGE followed by Coomassie blue staining and protein concentration was determined by Bradford assay with bovine serum albumin as a standard (Bradford, 1976). Protein was stored at −80 °C after concentrating the protein to about 10 mg mL^{-1} with an Amicon-Y5 membrane concentrator (Millipore).

Functional assay

Insulin reduction assays to assess SjTrx as reductant and its functional interaction with SjTGR were performed by following corresponding methods, respectively.

Stock insulin solution was prepared as described previously by Holmgren (Holmgren, 1979). Insulin was dissolved in Tris-HCl buffer at pH 8·0, then acidified to pH 2–3 by addition of 1·0 M HCl and back to pH 8·0 rapidly with 1·0 M NaOH. The final concentration was 10 mg mL^{-1} and the solution was clear and stored at −20 °C.

Freshly solutions including 5 mg mL^{-1} insulin in 0·1 M potassium phosphate (pH 7·4), 20 mM EDTA and 100 mM dithiothreitol (DTT) were stored in ice bath. The insulin reduction assay was performed by mixing 60 μL insulin, 30 μL EDTA, 4·0 or 8·0 μM SjTrx-S_2, and the potassium phosphate buffer to give a final volume of 300 μL. DTT (15 μL) was added to cuvettes and started the reaction except the blank. The direct reduction of insulin by DTT without Trx was recorded as a control cuvette. Cuvettes were placed in the spectrophotometer and the absorbance at 650 nm was measured every 1 min.

To assess the functional interaction of SjTrx with SjTGR, the insulin reduction assay was performed in the presence of NADPH and SjTGR by measurement of absorbance at 340 nm to monitor NADPH consumptions. SjTGR was added to the mixture containing 50 mM K-phosphate pH 7·4, 200 μM NADPH, 1 mg mL^{-1} insulin, 2 mM EDTA and 9 μM SjTrx.

Crystallization

Crystallization conditions were initially tested using Hampton kit of HR2-144 and then refined according to standard hanging drop methods. The best crystal of SjTrx grew over 3 days to maximum dimensions of 0·3 × 0·2 × 0·1 mm^3 (Fig. 1) in a drop composed of 2 μL protein (10 mg mL^{-1}) and 2 μL well solution of 30% PEG3350, 50 mM Bistris pH 6·5 and 10 mM $BaCl_2$.

X-ray data collection and processing

Crystals were cryoprotected with the same reservoir solution supplemented with 25% glycerol and vitrified by plunging crystals into liquid nitrogen directly. Data were collected at 100 K. The best dataset was collected as 1·0° oscillation frames using the ADSC Q315r CCD detector on the BL17U1 beamline at Shanghai Synchrotron Radiation Facility (SSRF, China) at a wavelength of 0·9707 Å. Data analysis performed with HKL2000 indicated that the crystal belongs to the $C222_1$ space group with dimensions of unit cell: $a = 90{\cdot}765$ Å; $b = 149{\cdot}364$ Å; $c = 39{\cdot}881$ Å; $\alpha = \beta = \gamma = 90$ °C (Otwinowski and Minor, 1997). Data were scaled at 2·0 Å resolutions, with an R_{merge} of 7·2% and a completeness of 99·8% (Table 1).

Structure refinement and analysis

The structure was solved by an automated molecular replacement pipeline of Balbes based on the best model with the identity of 0·642 (PDB accession: 2XBI) searched by program. Atomic coordinates and displacement parameters were refined using Phenix (Adams *et al*. 2010; Long *et al*. 2008). Model building and adjustments were carried out using the program package COOT (Emsley and Cowtan, 2004). The structure was refined to 2·0 Å resolution and the geometry was verified using PROCHECK (Laskowski *et al*. 1993). Statistics for the final refined model is given in Table 1. Atomic coordinates and structure factors have been deposited in the Protein Data Bank with the accession code 4I8B. Figures were prepared with the program PyMOL (http://www.pymol.org).

RESULTS

Cloning and preparation of SjTrx

The full-length cDNA sequence encoding SjTrx was amplified by PCR from cDNA library that was prepared using the RT-PCR method (Hu *et al*. 2003; Lu *et al*. 2012). Sequence analysis yielded a full-length cDNA containing an open reading frame (ORF) of 318 bp, which encode a protein of 106 amino acid residues with a calculated molecular weight of about 12 kDa and isoelectric point of 5·4. The highly conserved Trx active site motif of W33–C34–G35–P36–C37 was present in SjTrx, in which thiols in residues C34, C37 were reversible switched between sulphydryl and disulphide bond under the reduction and oxidation states.

The gene of SjTrx was cloned into the expression vector of pET28a and transformed into *E. coli* BL21 (DE3) strain. A recombinant protein containing an N-terminal six-histidine tag was expressed successfully with the molecular weight of about 12 kDa (Fig. 1). The supernatant of the lysate contained the majority of the target protein and the protein was purified using the His-tag affinity column and subsequently DEAE-sepharose ion-exchange column. The purified SjTrx protein was analysed by SDS-PAGE and the expected band was detected at ~12 kDa (Fig. 1). The protein sample was concentrated to about 10 mg mL^{-1} with Amicon-Y5 membrane concentrator.

Both native and optimized SjTrx genes were expressed and detected using SDS-PAGE successfully. The protein yield expressed using native gene was lower than the optimized gene, however, the product of optimized gene was instable and formed white precipitate after concentration. Finally all the SjTrx protein was prepared using the native SjTrx gene.

Properties of SjTrx

Insulin reduction. Trx kept in the reduced state by the addition of DTT can catalyse the reduction of insulin, which leads to the cleavage of two interchain

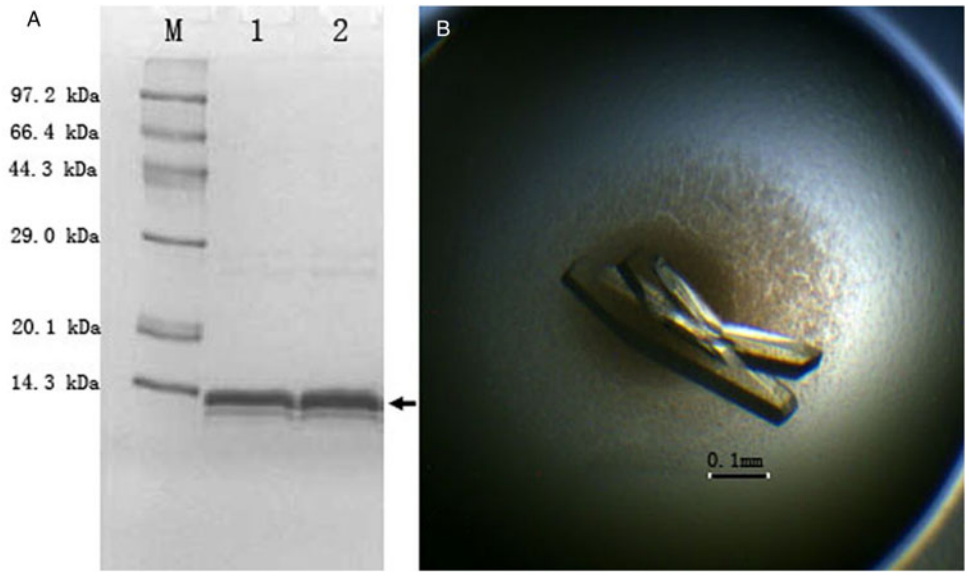

Fig. 1. Overexpression of the recombinant protein and the crystal image of SjTrx. Over expression of the recombinant protein and the crystal image of SjTrx. (A) 12% SDS-PAGE gel stained with Coomassie blue. Arrow indicates positions of the recombinant protein. Lane M, protein marker; Lanes 1 and 2, fractions of 6-Histag SjTrx from His-binding column; (B) A crystal of Trx from *S. japonicum* (SjTrx).

disulphide bridges in insulin (Holmgren, 1979). Turbidimetric assay at 650 nm was used to measure the white precipitation formed mainly from the insoluble free B chain of insulin (Sanger, 1949). Reduction reactions of insulin disulphides by DTT at pH 7·4 were determined in the presence and absence of SjTrx-S_2. Solutions containing a final concentration of 0·17 mM insulin (1·0 mg mL^{-1}) and 5 mM DTT were mixed and the SjTrx-S_2 protein was added to a final concentration of

Table 1. Summary of crystallography data

	SjTrx
Data collection	
Space group	$C222_1$
Cell dimension	
a, b, c (Å)[a]	90·756, 149·364, 39·881
α, β, γ(°)	90, 90, 90
Resolution range	50–2·0 (2·03–2·0)
R_{merge}	0·11 (0·641)
Mean I/sigma(I)	27·65 (6·54)
Completeness (%)	99·8 (98·7)
Redundancy	7·9 (6·8)
Refinement	
Resolution (Å)	2·0
Number of reflections	18888 (1819)
R-factor	0·1826 (0·2197)
R-free	0·2149 (0·2712)
Number of molecules in asymmetric unit	2
Number of atoms (2 monomer/au)	
Protein	1659
Water	122
B-factors (overall)	47·5
Ramachandran plot % of residues in	
Preferred regions	96·57
Allowed regions	3·43
Outliers	0
RMS deviations	
Bond lengths (Å)	0·007
Bond angles (°)	0·99

[a] Values within parentheses refer to the highest-resolution shell.

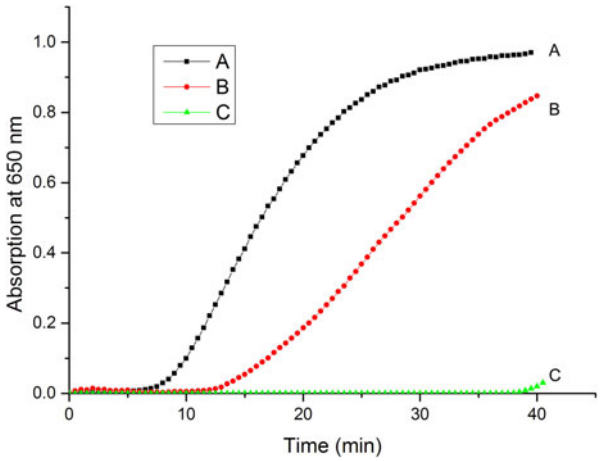

Fig. 2. Enzyme activity analysis of the recombinant SjTrx. (A) Reactions (in triplicate) with 8 μM recombinant *S. japonicum* thioredoxin (square); (B) 4 μM recombinant *S. japonicum* thioredoxin (dot); (C) only DTT without thioredoxin served as control (triangle). The absorbance at 650 nm is plotted against time, all with 5 mM DTT.

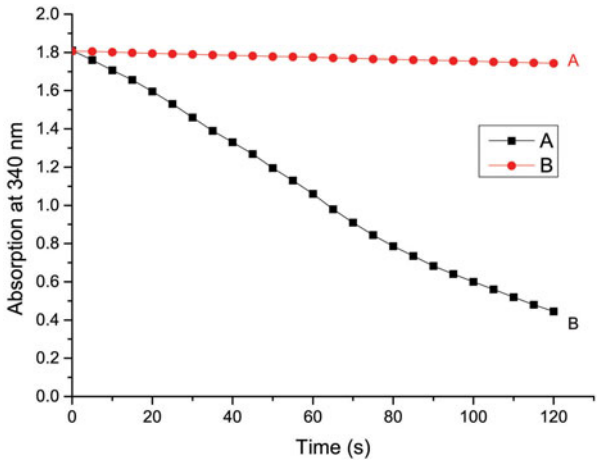

Fig. 3. TrxR activity with substrate of SjTrx. (A) TrxR assay was performed in solution containing 50 mM K-phosphate, pH 7·4, 200 mM NADPH, 1 mg mL^{-1} insulin, 2 mM EDTA, 9 μM SjTrx, 10 μL SjTGR and monitored the absorbance change at 340 nm. Absorption decreases due to conversion NADPH to NADP were measured as TR activity; (B) Control trial without SjTrx and insulin.

8·0 μM and 4·0 μM, respectively. Compared with the lower concentration of SjTrx-S_2 (4·0 μM), the presence of the higher concentration of SjTrx-S_2 (8·0 μM) resulted in the faster turbidity appearance corresponding to faster rate of precipitation (Fig. 2). The control cuvette without SjTrx, no precipitation was observed until 40 min late, however, the same amount of the final white precipitate was obtained in the cuvettes after incubation overnight regardless of SjTrx addition or not. Different equilibrium times indicated that SjTrx catalysed the DTT reduction of insulin disulphides.

Interaction with SjTGR. The coupling reaction among SjTGR, NADPH, SjTrx and insulin was used to assess the functional interaction of SjTrx with its endogenous reductase, selenocysteine SjTGR (SEC-SjTGR) (Kuntz *et al.* 2007; Song *et al.* 2012). The reduction assay was determined by monitoring the decrease of NADPH consumption at 340 nm. Results showed that SjTGR possessed the TrxR activity and the specific activity was 4·1 ± 0·07 μmol min^{-1} mg^{-1} with the substrate of SjTrx (Fig. 3). The enzyme assay of the recombinant SjTrx proved to be fully functional, consistent with the results published previously (Song *et al.* 2012).

Structure of SjTrx

There are two molecules per asymmetric unit, with a corresponding crystal volume per protein mass (V_M) of 2·83 Å^3 Da^{-1} and a solvent fraction of 56·62%. The structure (molecule A) of the oxidized SjTrx is shown in Fig. 4. Residues from 2 to 106 are clearly defined from electron density map. All residues fit map well except the C-terminal regions of residues 101–106 in molecule B. The SjTrx conserves the typical Trx fold, highly similar to the SmTrx (Trx from *Schistosoma mansoni*) (Boumis *et al.* 2011). In detail, the core region is consisting of one five-stranded β sheet (β1–5) surrounding by four α helices (α1 and α3, α2 and α4). The typical active site motif W33–C34–G35–P36–C37 is arranged in a β-turn shape, residing between the β2 strand and the α2 helix. Two thiols from Cys34 and Cys37 were oxidized to form one disulphide bridge with S–S bond length of 2·05 Å. There are no cysteine residues in SjTrx outside the active site, same as SmTrx (Boumis *et al.* 2011), but different from many other eukaryotic Trx (Alger *et al.* 2002).

The redox active cystine pair is covered largely by the C-terminal portion of helix α2 for Cys37 (Fig. 4) and solvent around residues Cys34 and Cys37. In addition, C34, Cys37 and its disulphide bond is partly shielded by the loop between β2 and α2, the N-terminus of the helix α2, and the C-terminal part of the α3–β4 loop. As a result of this arrangement, one side of the Cys34 sulphydryl group acts as the nucleophilic Cys for its substrates and is responsible for transferring reducing equivalents. As a resolving Cys, the Cys37 is shielded and deprotonated with the aid of one conserved Asp residue (Asp28) and an H-bond water molecule (Asp28 (OD1)-O = 2·82 Å) during the reaction of redox (Fig. 4). This notion is supported by the structure of *E. coli* TrxR-Trx (Lennon *et al.* 2000). Model study predicted that SjTGR and SjTrx forms interaction partner (Angelucci *et al.* 2010).

Alignment of the SjTrx sequence with those from other organisms shows a different identity from 34% (*Escherichia coli* and Human TRXL-N), 41%

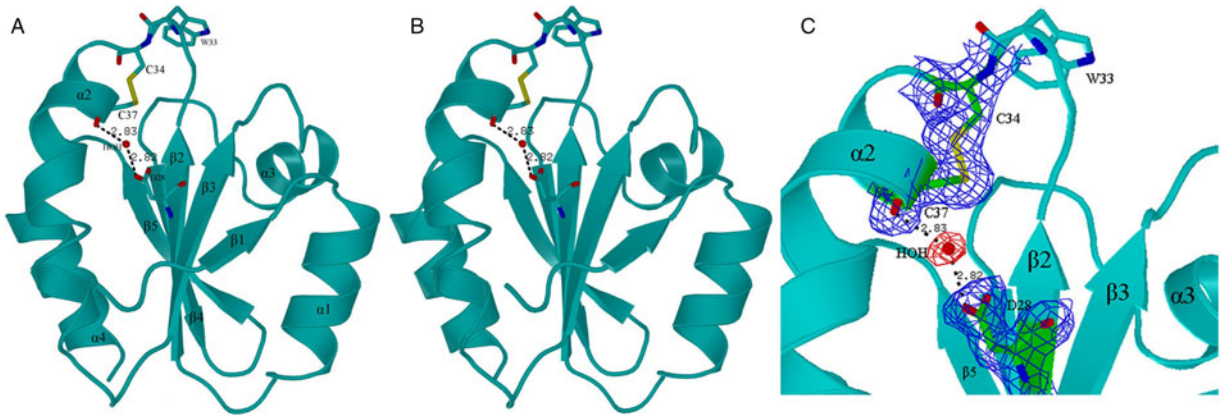

Fig. 4. Stereo cartoon representation of the overall structure of the oxidized SjTrx (A and B) and the enlarged view of the active site (C). Residues of the active site (Asp28, Trp33, Cys34 and Cys37) are in stick representation, together with the water molecule putatively involved in catalysis. The electron density $2F_0$–Fc contoured at $1{\cdot}5\sigma$ is also shown for the same residues. Hydrogen bonds are represented as dotted lines.

(*Plasmodium falciparum*), 43% (Human Trx), 47% (*Fasciola hepatica*), to 64% (*S. mansoni*) (Fig. 5). The overall rmsds between SjTrx and other species Trx range from 0·81 to 1·17 Å, showing the similarity in three-dimensional structures (Table 2). The comparison of two schistosome species Trx, such as SjTrx and SmTrx, reveals the high similarity in structural architecture (overall rmsd of 0·81 Å). Superimposition of their active site motif WCGPC shows a slight but detectable change (rmsd of 0·362 Å), smaller than the overall rmsd value of 0·81 Å. The significant differences between SjTrx and SmTrx occur primarily in the N-terminal β sheet formed by initial 7 residues (Fig. 6 and Table 3).

DISCUSSION

Trx, which reduces disulphides on target proteins, plays a central role in a variety of cellular redox reactions (Cheng *et al*. 2011). In the thiol-mediated detoxifying system, Trx has been proposed to be a

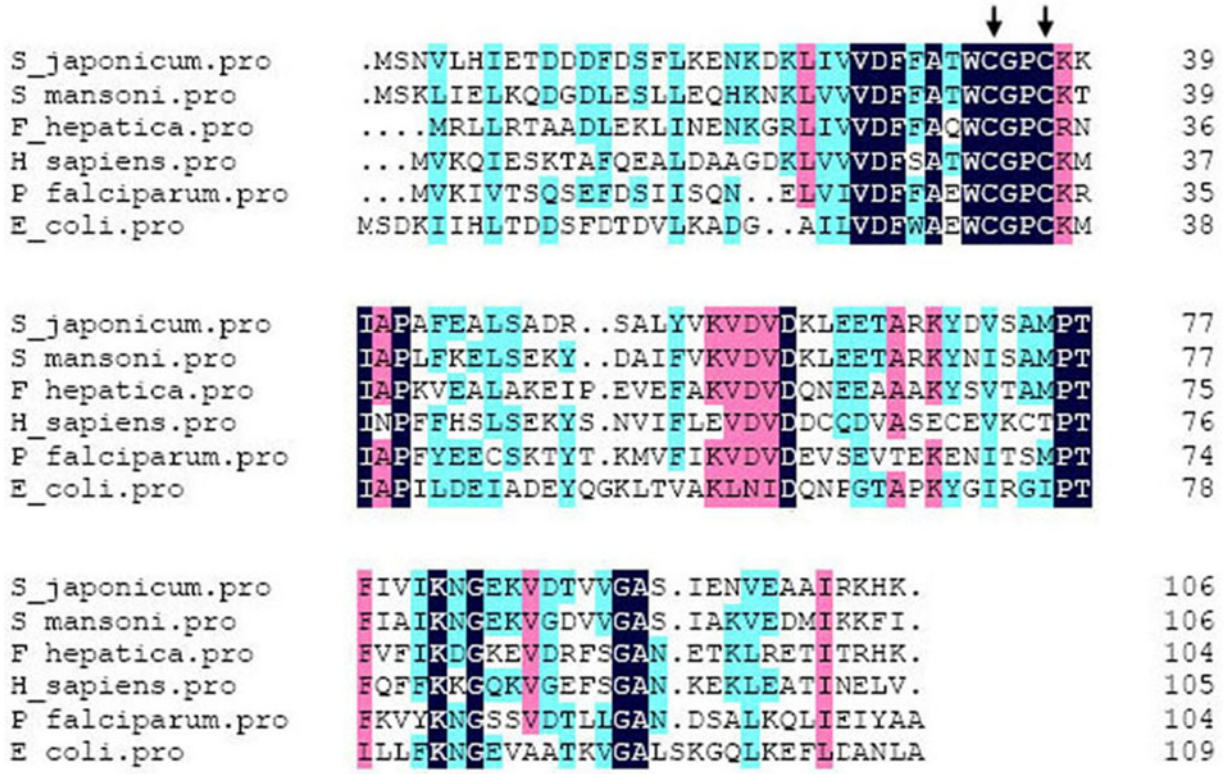

Fig. 5. Alignment of the thioredoxin amino acid sequence from *S. japonicum* with thioredoxins from other organisms: *S. mansoni* (AAL79841); *F. hepatica* (AAF14217); human thioredoxin (AAA74596); *P. falciparum* (AAF34541); *E. coli* (AAA24693). Arrow heads mark cysteine residues of the active site. Dots introduce to obtain the best alignment.

Table 2. Sequence identity and rmsd deviations of the representative structure compared with Thioredoxin from *S. japonicum* (SjTrx)

Protein structure	PDB ID	Sequence identity (%)	rmsd
Oxidized *S. mansoni* Trx	2XBI	64	0·81 Å
Oxidized *F. hepatica* Trx	2VIM	47	1·13 Å
Oxidized human Trx	1ERU	43	1·05 Å
Oxidized *P. falciparum* Trx	1SYR	41	1·10 Å
Oxidized *E. coli* Trx	2TRX	34	1·11 Å

crucial protein for parasite survival and the pathogens expressed throughout all life stages of schistosomes (Alger *et al*. 2002). In order to undertake a systematic study for the Trx involved redox system, in the first step we studied the structure and function of Trx. In the present study, Trx from *S. japonicum* (SjTrx) was shown to have the oxidoreductase activities of insulin reduction and to interact with endogenetic enzyme SjTGR, regulating the redox balance in schistosomes. In mammal redox regulations, Trx executes the redox reaction by oxidation of active site thiols and is then reduced by NADPH bound in the TrxR (Lennon *et al*. 2000; Jonsson *et al*. 2008), however, in schistosomes, the reduction of Trx is undertaken by a special TGR protein. Our crystal structure of SjTrx was demonstrated to be closely similar to the Trx from other species including human. In this aspect, the Trx may not be a good drug target because the cross-inhibition to human Trx may lead to severe side effects. However, the interacting proteins with Trx may be significantly different to allow developing a specific drug to disrupt the interactions of Trx with its protein partner.

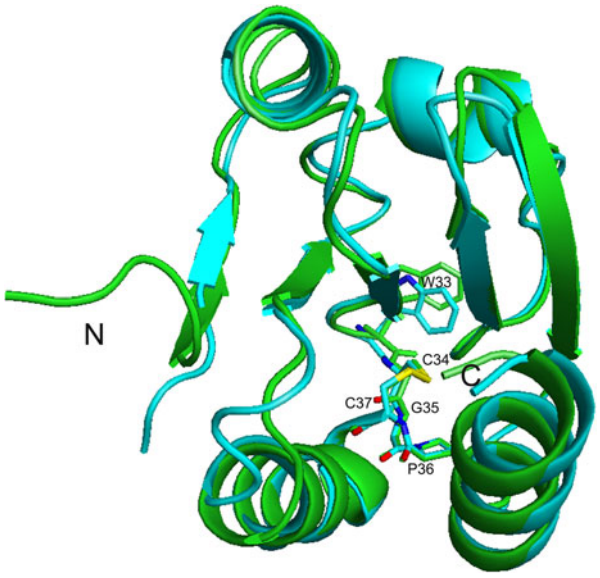

Fig. 6. Backbone superposition of SjTrx and SmTrx (residues 8–106). Active site residues shown in stick. SjTrx and SmTrx are coloured in cyan and chlorine, respectively.

Trx is a well-known multi-functional protein regulating the structure and activity of proteins in a wide array of processes including cell division, transcription regulation, energy transduction, and especially oxidative stress response (Arner and Holmgren, 2000; Kumar *et al*. 2004). In these regulations, apart from the oxidoreductase activity, Trx regulations of target proteins activity can be accomplished by two mechanisms. The first regulatory mechanism depends on the reversible thiol--disulphide exchange reactions between Trx and the target proteins containing regulatory cysteines (Hayashi *et al*. 1993; Schenk *et al*. 1994; Schurmann, 2003). Another mechanism depends on the interaction of Trx with target protein to form protein complexes (Richardson, 1983; Russel and Model, 1985; Liu *et al*. 2000). In the next step, we will systematically undertake the structural and functional studies of the Trx mediated redox pathway, especially the complexes of Trx with its partner proteins. To understand the precise mechanism of schistosome redox metabolism and how different it is from human one, more protein complex structures between SjTrx and its target protein or chemical inhibitors will be needed.

Recently, in human, an endogenous inhibitor of Trx, Trx-interacting protein, was identified and its complex structure was solved (Ishrat *et al*. 2014). It will be interesting to know whether a similar system exists in schistosome and how different this is from the human one. In *S. japonicum*, apart from the 12 kDa Trx, 32 kDa Trx-related protein (TRP32 protein) called SjTrx-1 has been cloned. SjTrx-1 express in all stages of parasite life cycle and the enzyme assay also shows the insulin reduction activity *in vitro* (Liu Jian *et al*. 2012). Most of proteins evolutionarily related to Trx catalyse formation of disulphide bonds in various proteins and belong to the protein-disulphide isomerase (PDI) family. These molecules contain one or more Trx domain in N-terminal and one proteasome-interacting Trx domain (PITH) in C-terminal (Holmgren, 1984; Lee *et al*. 1998; Andersen *et al*. 2009). Comparison of SjTrx-1 and SjTrx from *S. japonicum* shows significant differences in protein sequence (12·5% identity in whole; 33·6% identity in Trx domain) and molecular weight

Table 3. RMSD deviation of partial residues alignment of SjTrx and SmTrx

Residues range	Superposition form	rmsd
1–7	Backbone	1·23 Å
1–7	Overall	1·35 Å
8–106	Backbone	0·69 Å
8–106	Overall	0·79 Å

(SjTrx: 12 kDa; SjTrx-1: 32 kDa) but similarities in Trx activity *in vitro*.

ACKNOWLEDGEMENTS

The authors thank Dr Zhipu Luo from FJIRSM for help of synchrotron data collection.

FINANCIAL SUPPORT

The authors are grateful to the National Science Foundation of China (31260206, 30860073, 21405023), Natural Science Foundation of Jiangxi Province (20142B213008), General Financial Grant from the China Postdoctoral Science Foundation (2012M520352), Fund for Jiangxi 'Jinggang Star' Young Scientist Training Program (2011BCB23026) for financial support.

REFERENCES

Adams, P. D., Afonine, P. V., Bunkoczi, G., Chen, V. B., Davis, I. W., Echols, N., Headd, J. J., Hung, L. W., Kapral, G. J., Grosse-Kunstleve, R. W., Mccoy, A. J., Moriarty, N. W., Oeffner, R., Read, R. J., Richardson, D. C., Richardson, J. S., Terwilliger, T. C. and Zwart, P. H. (2010). PHENIX: a comprehensive Python-based system for macromolecular structure solution. *Acta Crystallographica, Section D (Biological Crystallography)* **66**, 213–221.

Alger, H. M. and Williams, D. L. (2002). The disulfide redox system of *Schistosoma mansoni* and the importance of a multifunctional enzyme, thioredoxin glutathione reductase. *Molecular and Biochemical Parasitology* **121**, 129–139.

Alger, H. M., Sayed, A. A., Stadecker, M. J. and Williams, D. L. (2002). Molecular and enzymatic characterisation of *Schistosoma mansoni* thioredoxin. *International Journal of Parasitology* **32**, 1285–1292.

Andersen, K. M., Madsen, L., Prag, S., Johnsen, A. H., Semple, C. A., Hendil, K. B. and Hartmann-Petersen, R. (2009). Thioredoxin Txnl1/TRP32 is a redox-active cofactor of the 26 S proteasome. *Journal of Biological Chemistry* **284**, 15246–15254.

Angelucci, F., Dimastrogiovanni, D., Boumis, G., Brunori, M., Miele, A. E., Saccoccia, F. and Bellelli, A. (2010). Mapping the catalytic cycle of *Schistosoma mansoni* thioredoxin glutathione reductase by X-ray crystallography. *Journal of Biological Chemistry* **285**, 32557–32567.

Arner, E. S. and Holmgren, A. (2000). Physiological functions of thioredoxin and thioredoxin reductase. *European Journal of Biochemistry* **267**, 6102–6109.

Boumis, G., Angelucci, F., Bellelli, A., Brunori, M., Dimastrogiovanni, D. and Miele, A. E. (2011). Structural and functional characterization of *Schistosoma mansoni* Thioredoxin. *Protein Science* **20**, 1069–1076.

Bradford, M. M. (1976). A rapid and sensitive method for the quantitation of microgram quantities of protein utilizing the principle of protein-dye binding. *Analytical Biochemistry* **72**, 248–254.

Butterworth, A. E. (1984). Cell-mediated damage to helminths. *Advance in Parasitology* **23**, 143–235.

Capron, M. and Capron, A. (1986). Rats, mice and men – models for immune effector mechanisms against schistosomiasis. *Parasitology Today* **2**, 69–75.

Cheng, Z., Zhang, J., Ballou, D. P. and Willams Jr, C. H. (2011). On the reactivity of thioredoxin as a protein thiol-disulfide oxidoreductase. *Chemical Reviews* **111**(9), 5768–5783.

Emsley, P. and Cowtan, K. (2004). Coot: model-building tools for molecular graphics. *Acta Crystallographica, Section D (Biological Crystallography)* **60**, 2126–2132.

Han, Y., Zhang, M., Hong, Y., Zhu, Z., Li, D., Li, X., Fu, Z. and Lin, J. (2012). Characterization of thioredoxin glutathione reductase in *Schistosoma japonicum*. *Parasitology International* **61**, 475–480.

Hatahet, F. and Ruddock, L. W. (2009). Protein disulfide isomerase: a critical evaluation of its function in disulfide bond formation. *Antioxidants and Redox Signaling* **11**, 2807–2850.

Hayashi, T., Ueno, Y. and Okamoto, T. (1993). Oxidoreductive regulation of nuclear factor kappa B. Involvement of a cellular reducing catalyst thioredoxin. *Journal of Biological Chemistry* **268**, 11380–11388.

Holmgren, A. (1979). Thioredoxin catalyzes the reduction of insulin disulfides by dithiothreitol and dihydrolipoamide. *Journal of Biological Chemistry* **254**, 9627–9632.

Holmgren, A. (1984). Enzymatic reduction–oxidation of protein disulfides by thioredoxin. *Methods in Enzymology* **107**, 295–300.

Hu, W., Yan, Q., Shen, D. K., Liu, F., Zhu, Z. D., Song, H. D., Xu, X. R., Wang, Z. J., Rong, Y. P., Zeng, L. C., Wu, J., Zhang, X., Wang, J. J., Xu, X. N., Wang, S. Y., Fu, G., Zhang, X. L., Wang, Z. Q., Brindley, P. J., Mcmanus, D. P., Xue, C. L., Feng, Z., Chen, Z. and Han, Z. G. (2003). Evolutionary and biomedical implications of a *Schistosoma japonicum* complementary DNA resource. *Nature Genetics* **35**, 139–147.

Ishrat, T., Mohamed, I. N., Pillai, B., Soliman, S., Fouda, A. Y., Ergul, A., El-Remessy, A. B. and Fagan, S. C. (2014). Thioredoxin-interacting protein: a novel target for neuroprotection in experimental thromboembolic stroke in mice. *Molecular Neurobiology*.Epub ahead of print, doi:10.1007/s12035-014-8766-x.

Jensen, K. S., Hansen, R. E. and Winther, J. R. (2009). Kinetic and thermodynamic aspects of cellular thiol-disulfide redox regulation. *Antioxidants and Redox Signaling* **11**, 1047–1058.

Jonsson, T. J., Johnson, L. C. and Lowther, W. T. (2008). Structure of the sulphiredoxin-peroxiredoxin complex reveals an essential repair embrace. *Nature* **451**, 98–101.

Kaimul Ahsan, M., Nakamura, H., Tanito, M., Yamada, K., Utsumi, H. and Yodoi, J. (2005). Thioredoxin-1 suppresses lung injury and apoptosis induced by diesel exhaust particles (DEP) by scavenging reactive oxygen species and by inhibiting DEP-induced downregulation of Akt. *Free Radical Biology and Medicine* **39**, 1549–1559.

Kazura, J. W., Fanning, M. M., Blumer, J. L. and Mahmoud, A. A. (1981). Role of cell-generated hydrogen peroxide in granulocyte-mediated killing of schistosomula of *Schistosoma mansoni in vitro*. *Journal of Clinical Investigation* **67**, 93–102.

Kumar, J. K., Tabor, S. and Richardson, C. C. (2004). Proteomic analysis of thioredoxin-targeted proteins in *Escherichia coli*. *Proceedings of National Academy of Sciences of the United States of America* **101**, 3759–3764.

Kuntz, A. N., Davioud-Charvet, E., Sayed, A. A., Califf, L. L., Dessolin, J., Arner, E. S. and Williams, D. L. (2007). Thioredoxin glutathione reductase from *Schistosoma mansoni*: an essential parasite enzyme and a key drug target. *PLoS Medicine* **4**, e206.

Laskowski, R. A., Macarthur, M. W., Moss, D. S. and Thornton, J. M. (1993). PROCHECK: a program to check the stereochemical quality of protein structures. *Journal of Applied Crystallography* **26**, 283–291.

Lee, K. K., Murakawa, M., Takahashi, S., Tsubuki, S., Kawashima, S., Sakamaki, K. and Yonehara, S. (1998). Purification, molecular cloning, and characterization of TRP32, a novel thioredoxin-related mammalian protein of 32 kDa. *Journal of Biological Chemistry* **273**, 19160–19166.

Lennon, B. W., Williams, C. H., Jr. and Ludwig, M. L. (2000). Twists in catalysis: alternating conformations of *Escherichia coli* thioredoxin reductase. *Science* **289**, 1190–1194.

Lillig, C. H. and Holmgren, A. (2007). Thioredoxin and related molecules – from biology to health and disease. *Antioxidant and Redox Signal* **9**, 25–47.

Liu, H., Nishitoh, H., Ichijo, H. and Kyriakis, J. M. (2000). Activation of apoptosis signal-regulating kinase 1 (ASK1) by tumor necrosis factor receptor-associated factor 2 requires prior dissociation of the ASK1 inhibitor thioredoxin. *Molecular and Cellular Biology* **20**, 2198–2208.

Liu Jian, X. B., Zhang, X., Liu, L., Hu, W., Wang, X.-N. (2012). Cloning, expression and function analysis of thioredoxin-1 protein of *Schistosoma japonicum*. *Chinese Journal of Parasitology and Parasitic Diseases* **30**, 335–340.

Long, F., Vagin, A. A., Young, P. and Murshudov, G. N. (2008). BALBES: a molecular-replacement pipeline. *Acta Crystallographica, Section D (Biological Crystallography)* **64**, 125–132.

Loverde, P. T. (1998). Do antioxidants play a role in schistosome host–parasite interactions? *Parasitology Today* **14**, 284–289.

Lu, Y., Xu, B., Ju, C., Mo, X. J., Chen, S. B., Feng, Z., Wang, X. N. and Hu, W. (2012). Immunoscreening of *Schistosoma japonicum* egg cDNA library and identification of positive clones. *Zhongguo Ji Sheng Chong Xue Yu Ji Sheng Chong Bing Za Zhi* **30**, 109–115.

Michelet, L., Zaffagnini, M., Marchand, C., Collin, V., Decottignies, P., Tsan, P., Lancelin, J. M., Trost, P., Miginiac-Maslow, M., Noctor, G. and Lemaire, S. D. (2005). Glutathionylation of chloroplast thioredoxin f is a redox signaling mechanism in plants. *Proceedings of National Academy of Sciences of the United States of America* **102**, 16478–16483.

Otwinowski, Z. and Minor, W. (1997). Processing of x-ray diffraction data collected in oscillation mode. *Methods in Enzymology* **276**, 307–326.

Powis, G. and Montfort, W. R. (2001). Properties and biological activities of thioredoxins. *Annual Review of Pharmacology and Toxicology* **41**, 261–295.

Puigbo, P., Guzman, E., Romeu, A. and Garcia-Vallve, S. (2007). OPTIMIZER: a web server for optimizing the codon usage of DNA sequences. *Nucleic Acids Research* **35**, W126–W131.

Puigbo, P., Romeu, A. and Garcia-Vallve, S. (2008). HEG-DB: a database of predicted highly expressed genes in prokaryotic complete genomes under translational selection. *Nucleic Acids Research* **36**, D524–D527.

Richardson, C. C. (1983). Bacteriophage T7: minimal requirements for the replication of a duplex DNA molecule. *Cell* **33**, 315–317.

Russel, M. and Model, P. (1985). Thioredoxin is required for filamentous phage assembly. *Proceedings of National Academy of Sciences of the United States of America* **82**, 29–33.

Ryter, S. W. and Tyrrell, R. M. (2000). The heme synthesis and degradation pathways: role in oxidant sensitivity. Heme oxygenase has both pro- and antioxidant properties. *Free Radical and Biological Medicine* **28**, 289–309.

Sanger, F. (1949). Fractionation of oxidized insulin. *Biochemical Journal* **44**, 126–128.

Schenk, H., Klein, M., Erdbrugger, W., Droge, W. and Schulze-Osthoff, K. (1994). Distinct effects of thioredoxin and antioxidants on the activation of transcription factors NF-kappa B and AP-1. *Proceedings of National Academy of Sciences of the United States of America* **91**, 1672–1676.

Schurmann, P. (2003). Redox signaling in the chloroplast: the ferredoxin/thioredoxin system. *Antioxidant and Redox Signal* **5**, 69–78.

Song, L., Li, J., Xie, S., Qian, C., Wang, J., Zhang, W., Yin, X., Hua, Z. and Yu, C. (2012). Thioredoxin glutathione reductase as a novel drug target: evidence from *Schistosoma japonicum*. *PLoS One* **7**, e31456.

Wahl, M. C., Irmler, A., Hecker, B., Schirmer, R. H. and Becker, K. (2005). Comparative structural analysis of oxidized and reduced thioredoxin from *Drosophila melanogaster*. *Journal of Molecular Biology* **345**, 1119–1130.

WHO (2014). *Schistosomiasis Fact sheet N°115*. World Health Organization, Geneva, Switzerland.

Yoshioka, J., Schreiter, E. R. and Lee, R. T. (2006). Role of thioredoxin in cell growth through interactions with signaling molecules. *Antioxidant and Redox Signal* **8**, 2143–2151.